JOURNAL OF MATERIALS SCIENCE 30 (1995) 639–642

Calculated elastic constants of alumina–mullite ceramic particles

H. LEDBETTER
National Institute of Standards and Technology, Boulder, Colorado 80303, USA
M. DUNN
Mechanical Engineering Department, University of Colorado, Boulder, Colorado 80309, USA
M. COUPER
Comalco Research Centre, 15 Edgars Road, Thomastown, Victoria 3074, Australia

Using two theoretical models, we estimated the isotropic elastic constants of an alumina–mullite ceramic composite. The alumina phase, 20% by volume, consisted of brick-shaped particles with a 4:1 aspect ratio embedded in a mullite matrix (mullite= $3Al_2O_3{\cdot}2SiO_2$). We took alumina elastic-constant values from the literature, and we measured mullite's elastic constants using a megahertz-frequency pulse-echo method. The two theoretical models, Datta–Ledbetter and Mori–Tanaka, proceed from very different viewpoints. The Datta–Ledbetter model uses the long-wavelength limit of a scattered plane wave ensemble-average approach. The model estimates the speed of a plane harmonic wave, averages the scattered field by the Waterman–Truell procedure and uses Lax's quasicrystalline approximation to sum over pairs. The Mori–Tanaka method proceeds by estimating the average matrix stress in a material containing ellipsoidal inclusions. For randomly oriented ellipsoids, it extends Eshelby's solution for a single ellipsoidal inclusion. Both models lack adjustable parameters. Surprisingly, the two models with different physical approaches give practically identical results. A rough check on our estimates is that they lead to correct predictions of the elastic constants of an alumina–mullite-particle aluminium-matrix composite.

1. Introduction

Increasingly, new materials use small particles or fibres to achieve desired properties. Depending on the physical property, small dimensions present severe measurement problems. For example, for elastic constants, which are essential both for understanding and engineering a material, specimens below a few millimetres in size present severe difficulties for measurements by usual methods.

The present study focuses on small ($< 100\ \mu m$) ceramic composite spheres. Figs 1 and 2 show their microstructure. The spheres consist approximately of 20 vol% alumina (Al_2O_3) embedded in a mullite ($3Al_2O_3 \cdot 2SiO_2$) matrix. The alumina particles show a brick-type shape with an aspect ratio c/a estimated as 4:1.

Directly or indirectly measuring these particles' elastic constants presents a formidable problem; hence we adopted another approach: quantitative modelling. From the constituents' elastic constants, volume fractions and phase geometry, we calculated the macroscopic composite elastic constants.

We used two models: Datta–Ledbetter and Mori–Tanaka. Both models are described qualitatively in the abstract and in more detail below.

Because the reported mullite elastic constants are suspect, we measured a high-quality specimen using a megahertz-frequency pulse-echo superposition method that gives typical uncertainties of 1 in 1000. For alumina, we took reported monocrystal values and averaged them to effective polycrystal values by a Voigt–Reuss–Hill method.

Thus, the principal challenge of this study was to model the elastic constants of a ceramic–ceramic composite comprising 20% by volume of alumina short rods embedded in a mullite matrix.

2. Experimental procedure

Full details of the mullite elastic-constant measurements, including their remarkable temperature dependence, will appear elsewhere [1]. Briefly, we applied a pulse-echo superposition method, using 9 MHz x-cut and ac-cut transducers bonded with phenyl salicylate. We reflected ultrasonic waves from the flat and parallel surfaces of a polycrystalline specimen hot-pressed into a 0.8 cm × 1.8 cm × 3.0 cm rectangular parallelepiped. The macroscopic and X-ray diffraction mass densities were 3.156 and 3.168 $g\,cm^{-3}$, respectively. Table I shows the measured elastic con-

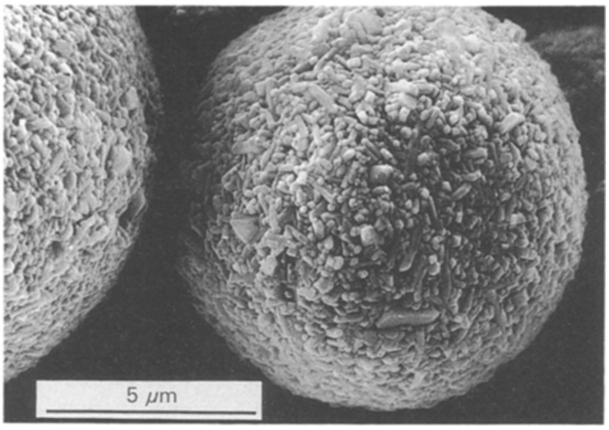

Figure 1 Typical alumina–mullite microsphere imaged by scanning electron microscopy.

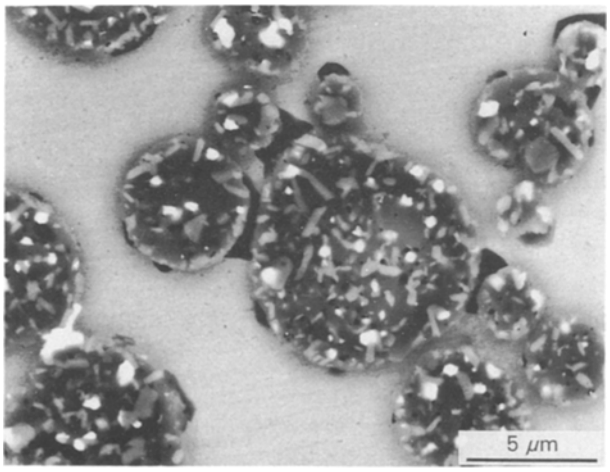

Figure 2 Several microspheres showing alumina phase (lighter) in mullite matrix (darker). Obtained by scanning electron microscopy. Bright white areas represent electrical-charge artefacts.

TABLE I Properties of constituents and composite calculation results

	α-Alumina	Mullite	Composite	
			D–L model	M–T model
$\rho(\mathrm{g\,cm^{-3}})$	3.986	3.168	3.332	3.332
B(GPa)	252.0	173.9	186.9	186.9
E(GPa)	402.9	229.1	256.4	256.3
G(GPa)	163.3	89.5	100.8	100.8
ν	0.234	0.280	0.271	0.271

stants. The table shows also alumina's effective polycrystalline constants obtained from Tefft's [2] monocrystal measurements and a Voigt–Reuss–Hill arithmetic average [3].

3. Results

Mathematical models of macroscopic–microscopic physical properties offer at least four principal uses:

1. Prediction of a mixture's macroscopic properties. Thus, one can predict a mixture's macroscopic response to field tensors such as stress and temperature.

2. Design: a rational approach to improve material properties to meet special needs.

3. A diagnostic tool. For example, for determining the volume fraction of a particle phase by measuring a macroscopic physical property.

4. Used inversely, to determine a particle's physical properties. For example: the elastic properties of particles formed *in situ*, particles not available separately for study, or particles too small for practical study.

3.1. The Datta–Ledbetter model

We used a scattered plane wave ensemble-average theory to estimate the elastic constants. Here we describe briefly the theory, which we discussed elsewhere in detail [4, 5] (the first reference is a full version, the second a simpler short version). First, we assume that the composite contains a random homogeneous distribution of ellipsoidal alumina particles in a homogeneous, isotropic mullite matrix. Second, we assume an incident plane wave with wavelength large compared with particle size. One expects the scattered wave to transmit through the material as a coherent plane wave with an effective wave speed v independent of propagation direction. The appropriate effective elastic stiffness is then $C = \rho v^2$, where ρ denotes mass density.

Ledbetter and Datta [4] showed that the wave speed follows from the governing dispersion relationship. This relationship was derived from a multiple-scattering formalism that makes two principal approximations:

1. A well-stirred distribution. With the first particle at R_1, the conditional probability density of a second particle at R_2 is

$$\begin{aligned} \rho(R_2|R_1) &= 1/V,\ |R_2 - R_1| \geqslant 2a \\ &= 0,\ |R_2 - R_1| < a \end{aligned} \quad (1)$$

Here, a denotes particle radius and V denotes volume.

2. The Lax quasicrystalline approximation

$$\langle u_j \rangle_{ji} = \langle u_j \rangle_j \quad (2)$$

Here, $\langle u_j \rangle_j$ represents the expectation value of the field quantity u_j keeping the jth particle fixed, and $\langle u_j \rangle_{ji}$ is the conditional expectation relative to the jth and ith particles.

A third, implicit, assumption is that an effective coherent plane wave moves through the composite medium with a characteristic wave speed, the effective wave speed.

The first approximation is somewhat restrictive and one expects its validity only for low particle concentrations. Generalizations to higher concentrations require appropriate correlation functions (for a discussion see Willis [6]). However, for simplicity we invoke this approximation for the present study. As described below for the present composite, theory matches observation closely. Thus, at least here, this simplifying approximation is valid, as it was in several previous studies involving high particle concentrations [4, 7, 8].

3.2. The Mori–Tanaka model

3.2.1. *Effective moduli of two-phase elastic composites*

General expressions for the effective elastic moduli of two-phase perfect-bond composites can be derived by considering over the composite the volume average of the stress $\boldsymbol{\sigma}_{ij}$ and strain $\boldsymbol{\varepsilon}_{ij}$:

$$\bar{\boldsymbol{\sigma}} = c_1\bar{\boldsymbol{\sigma}} + c_2\{\bar{\boldsymbol{\sigma}}_2\} \tag{3}$$

$$\bar{\boldsymbol{\varepsilon}} = c_1\bar{\boldsymbol{\varepsilon}} + c_2\{\bar{\boldsymbol{\varepsilon}}_2\} \tag{4}$$

In Equations 3 and 4 an overbar denotes the volume average of a quantity, braces { } denote the orientational average of an orientation- dependent quantity, and the well-known shorthand notation has been used for tensor quantities. Subscripts 1 and 2 denote the matrix and reinforcing phases, respectively, and c_i denotes the volume fraction of the ith phase, with $c_1 + c_2 = 1$. In each phase, ε and σ relate through Hooke's law: $\boldsymbol{\sigma}_i = \boldsymbol{C}_i\boldsymbol{\varepsilon}_i$. Consider that the two-phase composite is subjected to homogeneous displacement boundary conditions ε^0: $u_i^0(S) = \varepsilon_{ij}^0 x_j$ where S denotes the composite's surface. By homogeneous boundary conditions we mean that when they are applied to a homogeneous solid they result in homogeneous stress and strain fields. The volume-averaged stress and strain relate through effective elastic stiffnesses $\boldsymbol{C}$:

$$\bar{\boldsymbol{\sigma}} = \boldsymbol{C}\bar{\boldsymbol{\varepsilon}} \tag{5}$$

Noting that the perturbation of the strain field vanishes when integrated over the domain of the entire composite, $\bar{\boldsymbol{\varepsilon}}$ can be expressed as

$$\bar{\boldsymbol{\varepsilon}} = c_1\bar{\boldsymbol{\varepsilon}}_1 + c_2\{\bar{\boldsymbol{\varepsilon}}_2\} = \boldsymbol{\varepsilon}^0 \tag{6}$$

Equation 4 is a statement of the average strain theorem of elasticity for heterogeneous materials. Equations 3–6 can be combined to yield

$$\boldsymbol{C} = \boldsymbol{C}_1 + c_2\{(\boldsymbol{C}_2 - \boldsymbol{C}_1)\boldsymbol{A}\} \tag{7}$$

In Equation 7, $\boldsymbol{A}$ denotes the strain-concentration factor (fourth-order tensor) that relates the average strain in the reinforcing phase to that in the composite:

$$\bar{\boldsymbol{\varepsilon}}_2 = \boldsymbol{A}\bar{\boldsymbol{\varepsilon}} = \boldsymbol{A}\boldsymbol{\varepsilon}^0 \tag{8}$$

In general, $\boldsymbol{A}$ depends on orientation. Thus, estimating $\boldsymbol{A}$ is the key to predicting the effective elastic stiffnesses $\boldsymbol{C}$. In general, $\boldsymbol{A}$ cannot be obtained exactly and must be estimated by some approximate method.

3.2.2. *Estimates of the strain-concentration factor* **A**

The simplest approximations of $\boldsymbol{A}$ and $\boldsymbol{B}$ are $\boldsymbol{A} = \boldsymbol{I}$ and $\boldsymbol{B} = \boldsymbol{I}$, which are the Voigt [9] and Reuss [10] approximations, respectively. (Here $\boldsymbol{B}$ denotes the stress-concentration factor, an alternative way to solve the problem.) The next simplest estimate is the dilute approximation where the interaction among the reinforcing particles in a matrix-based composite is ignored. The concentration factor $\boldsymbol{A}$ is obtained from the solution of the auxiliary problem of a single particle embedded in an infinite matrix. For an ellipsoidal particle, Eshelby's [11] solution is most convenient and leads to the concentration factor for an isolated single inclusion, $\boldsymbol{A}^{\text{dil}}$:

$$\boldsymbol{A}^{\text{dil}} = [\boldsymbol{I} + \boldsymbol{S}\boldsymbol{C}_1^{-1}(\boldsymbol{C}_2 - \boldsymbol{C}_1)]^{-1} \tag{9}$$

Here $\boldsymbol{I}$ denotes the fourth-order identity tensor and $\boldsymbol{S}$ Eshelby's tensor (fourth order), which is a function only of the shape of the inclusion and the elastic constants of the matrix (Poisson's ratio for an isotropic matrix). Explicit expressions for $\boldsymbol{S}$ for many ellipsoidal shapes were tabulated by Mura [12]. Substitution of Equation 9 into Equation 7 yields an explicit expression for the effective elastic constants of the composite, an expression valid for dilute reinforcement concentrations.

One of the easiest methods available for considering interactions among reinforcing particles at higher concentrations is the Mori–Tanaka [13] mean-field theory. The original study of Mori and Tanaka focused on estimating the average internal stress in a matrix material containing precipitates with eigenstrains (transformation strains). Since then, the method has been applied successfully to many problems in the mechanics and physics of composite materials. Initially the method was linked with Eshelby's [11] equivalent-inclusion method as used by Takao *et al.* [14]; a review of many applications in this context was given by Taya and Arsenault [15]. Recently, Benveniste [16] reexamined the underlying assumptions of the method and reformulated it in a direct approach. The method has also received considerable attention from a theoretical standpoint (e.g. Chen *et al* [17] and references therein) and has been shown to be on strong theoretical footing for the elastic behaviour of two-phase composite media. In fact, for a two-phase elastic composite containing ellipsoidal inclusions, the Mori–Tanaka effective moduli coincide with Willis's [18] bounds (Weng [19]), which are an extension of the Hashin–Shtrikman bounds to include information on inclusion shape.

The key assumption in the Mori–Tanaka [13] theory is that the concentration factor $\boldsymbol{A}$ is given by the solution for a single particle embedded in an infinite matrix subjected to boundary conditions compatible with a strain field equal to the as-yet-unknown average strain in the matrix:

$$\bar{\varepsilon}_2 = \boldsymbol{A}^{\text{dil}}\bar{\varepsilon}_1 \tag{10}$$

Here $\boldsymbol{A}$ is given by Equation 9.

With Equations 6, 8 and 10, the concentration factor $\boldsymbol{A}^{\text{MT}}$ can be written

$$\boldsymbol{A}^{\text{MT}} = \boldsymbol{A}^{\text{dil}}[c_1\boldsymbol{I} + c_2\{\boldsymbol{A}^{\text{dil}}\}]^{-1} \tag{11}$$

Equation 11 was first obtained by Benveniste [16]. Equations 7 and 11 provide an explicit expression for the composite's effective elastic moduli:

$$\boldsymbol{C} = \boldsymbol{C}_1 + c_2\{(\boldsymbol{C}_2 - \boldsymbol{C}_1)\boldsymbol{A}^{\text{dil}}\}[c_1\boldsymbol{I} + c_2\{\boldsymbol{A}^{\text{dil}}\}]^{-1} \tag{12}$$

Here again, $\boldsymbol{A}^{\text{dil}}$ is given by Equation 9 and is a function of $\boldsymbol{C}_1$, $\boldsymbol{C}_2$ and $\boldsymbol{S}$. Equation 12 is an explicit equation for the effective elastic moduli; no iterative or other numerical schemes are required for its solution. A catalogue of simplified expressions for many extreme microstructural geometries was given by Chen *et al.* [17]. For composites with perfectly aligned reinforcements, the orientational averages in Equation 12 can be removed.

4. Discussion

The model-calculation results shown in Table I show several interesting features. First, although the two theoretical models approach the problem from very different viewpoints, and the material lies well beyond the dilute limit, the results are practically identical. This agreement confirms at least the calculations' mathematical correctness. Furthermore, it suggests the calculations' physical correctness. Second, all the calculated elastic properties lie between the bounds of the softer matrix and the stiffer particle. Third, all the calculated elastic stiffnesses (B, E, G)–lie well below a linear rule of mixtures and along a stiffness–concentration curve with positive curvature. Fourth, the Poisson's ratio lies slightly above a linear rule-of-mixture value, and thus along a curve with small negative curvature. (The mass density should follow exactly a linear rule of mixture. Thus we predict that the particle mass density equals 3.332 $\mathrm{g\,cm^{-3}}$.)

The particle aspect ratio ($c/a = 4$) produces little effect on the elastic constants. For example, for spheres ($c/a = 1$) the shear modulus equals 100.74 instead of 100.82 GPa. For prolate ellipsoid (rod-shape) particles, significant stiffening occurs only for much higher aspect ratios (see Datta and Ledbetter [20], especially Figs 5 and 6).

To test our results' veracity, we used them as input information to estimate the effective elastic constants of an alumina–mullite particle-reinforced aluminium-matrix composite. Using both resonance (kilohertz) and pulse-echo (megahertz) methods, we measured the Young's moduli of composites with seven volume fractions. (Full results of this study will appear elsewhere [21].) For a composite with 0.24 volume fraction of alumina–mullite particles we found $E = 96.1$, 94.6 and 93.3 GPa for the resonance, pulse-echo and calculation results, respectively. Other composites behaved comparably. Thus, this measurement–modelling agreement within 2% supports our calculated alumina–mullite elastic properties.

5. Conclusions

From this study we reached four conclusions:

1. We can calculate the effective quasi-isotropic elastic constants of a ceramic–ceramic composite where the occluded phase consists of short rods approximated as ellipsoids with $c/a = 4$. The particular example is α-alumina particles in a mullite matrix.

2. We found good agreement between two models: Datta–Ledbetter and Mori–Tanaka. The first is a long-wavelength-limit scattered plane wave ensemble-average approach. The second focuses on "average stress" in the matrix and Eshelby's solution of an ellipsoidal inclusion.

3. All the usual elastic stiffnesses–bulk, Young's and shear moduli–depart strongly negatively from a linear rule of mixtures.

4. Our estimates receive confirmation from the good agreement between measured and modelled Young's moduli of alumina–mullite particle-reinforced aluminium-matrix composites.

Acknowledgement

S. Kim (NIST) helped with both calculations and measurements.

References

1. H. LEDBETTER, S. KIM and W. KRIVEN, *J. Amer. Ceram. Soc. in press.*
2. W. TEFFT, *J. Res. Nat. Bur. Stands.* **70A** (1966) 277.
3. H. LEDBETTER, in "Dynamic Elastic-Modulus Measurements" (ASTM, Philadelphia, 1990) p. 135.
4. H. LEDBETTER and S. DATTA, *J. Acoust. Soc. Amer.* **79** (1986) 239.
5. *Idem, Z. Metallkde.* **83** (1992) 195.
6. J. WILLIS, in "Advances in Supplied Mechanics", Vol. 21 (Academic, New York, 1981) p. 1.
7. H. LEDBETTER and S. DATTA, *JSME Int. J.* **34** (1991) 194.
8. H. LEDBETTER and C. FORTUNKO, in "IEEE Ultrasonics Symposium" (IEEE, New York, 1991) p. 1065.
9. W. VOIGT, *Ann. Phys.* **38** (1889) 573.
10. A. REUSS, *Angew. Math. Mech.* **9** (1929) 49.
11. J. ESHELBY, *Proc. Roy. Soc.* **A241** (1957) 376.
12. T. MURA, "Micromechanics of Defects in Solids" (Nijhoff, The Hague, 1987) p. 77–84.
13. T. MORI and K. TANAKA, *Acta Metall.* **21** (1973) 571.
14. Y. TAKAO, T. CHOU and M. TAYA, *Trans. ASME* **49** (1982) 536.
15. M. TAYA and R. ARSENAULT, "Metal Matrix Composites, Thermomechanical Behavior" (Pergamon, Oxford, 1989) p. 32.
16. Y. BENVENISTE, *Mech. Mater.* **6** (1987) 147.
17. T. CHEN, G. DVORAK and Y. BENVENISTE, *J. Appl. Mech.* **59** (1992) 539.
18. J. WILLIS, *J. Mech. Phys. Solids* **25** (1977) 185.
19. G. WENG, *Int. J. Engng Sci.* **22** (1984) 845.
20. S. DATTA and H. LEDBETTER, in "Wave Propagation in Nonhomogeneous Media and Ultrasonic Nondestructive Evaluation" (ASME, New York, 1984) p. 123.
21. M. DUNN and H. LEDBETTER, *J. Appl. Mech. in press.*

Received 18 April
and accepted 10 May 1994